Powder Technology 433 (2024) 119172

Contents lists available at ScienceDirect

Powder Technology

journal homepage: www.journals.elsevier.com/powder-technology

Auto-agglomeration of dry ibuprofen powder under mechanical vibration: Effect of particle morphology and surface properties

Svetlana Bibiceva, Sven L.M. Schroeder, Ali Hassanpour *

School of Chemical and Process Engineering, University of Leeds, Leeds, United Kingdom

HIGHLIGHTS

- Particle morphology and surface properties impact auto-agglomeration of ibuprofen powder.
- Inverse correlation between auto-agglomeration and tribo-charging tendencies is seen.
- Undesirable auto-agglomeration appeared to be hindered by higher particle surface polarity.
- Higher surface polarity can be achieved by recrystallisation from polar solvent and/or induced by breakage.

GRAPHICAL ABSTRACT

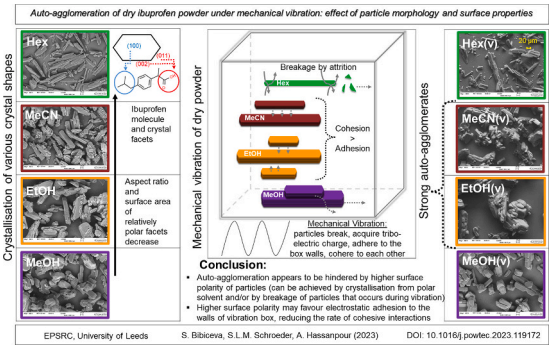

ARTICLE INFO

Keywords:
Auto-agglomeration
Ibuprofen
Tribo-electrification

ABSTRACT

This study investigates the effect of ibuprofen particle morphology and surface properties on its tendency to auto-agglomerate. Four diverse particle morphologies were produced by recrystallisation of ibuprofen from solvents with different polarities. The aspect ratio and the polar component of the recrystallised particles decreased as follows: methanol > ethanol > acetonitrile > hexane. The auto-agglomeration process was induced by mechanical vibration and the agglomerate strength was assessed by the Dispersion and Agglomerate Strength indices. Relatively strong agglomerates were detected only in the case of ibuprofen recrystallised from ethanol and acetonitrile, whereas weaker and no agglomerates were formed during mechanical vibration of ibuprofen recrystallised from methanol and hexane, respectively. It was found that tendency of ibuprofen powder to auto-agglomerate was associated with lower tribo-electric charges during mechanical vibration, hypothetically linked to the competitive advantage of electrostatic attraction of high surface polarity particles to the walls of the vibration box which can hinder particle-particle interactions. Crystal surface polarity could be altered by the crystallisation protocol and/or by particle breakage (exposing more crystal facets of high polarity) during mechanical vibration.

* Corresponding author.
E-mail address: a.hassanpour@leeds.ac.uk (A. Hassanpour).

https://doi.org/10.1016/j.powtec.2023.119172
Received 25 August 2023; Received in revised form 30 October 2023; Accepted 14 November 2023
Available online 19 November 2023

1. Introduction

The term auto-agglomeration in the context of dry Active Pharmaceutical Ingredient (API) powder refers to material sticking to itself that leads to the formation, and subsequent growth and/or strengthening of agglomerates - assemblages of bound primary API crystals and their fragments [1]. A dry API may undergo auto-agglomeration during various stages of the drug manufacturing process, including powder mixing, blending, milling, handling, transportation and/or storage [2–8]. The prefix "auto" is used to emphasise the fact that the discussed phenomenon occurs without any additives. Its occurrence is generally considered undesirable. Relatively soft API auto-agglomerates may regularly form during powder processing, but these are likely to be broken without any additional measures taken. Formation of hard API agglomerates that withstand breakage during the manufacturing process may lead to an inadequate API distribution within final product formulations, negatively impacting the API dissolution profile and its bioavailability. They may also impact powder flowability and compressibility creating risks with safety as well as efficacy and processability of the drug product [3,5,9–12].

Despite the crucial role API auto-agglomeration may play in drug product manufacturing and performance, the number of studies addressing dry API powder auto-agglomeration is limited and its underlying root-causes remain largely unknown. The reported papers are mostly on wet/moist API material agglomeration taking place during its crystallisation and subsequent drying [8,12,13] as well as those on non-API dry materials, such as inorganic chemicals [14,15], detergents [16] and food powders [17,18] and, in addition, on other types of unwanted dry powder transformation, including bulk powder caking [19,20].

In principle, there are many factors, both intrinsic and extrinsic, that need to be considered when studying auto-agglomeration of dry API powders. The intrinsic properties of the primary particles, such as particle size, morphology, surface energy, surface roughness, amorphous content, and many others, along with the interparticle forces heavily affect powder behaviour. Interparticle forces include chemical bonding, van der Waals interactions, solid bridges, liquid bridges, and electrostatics. When they are attractive particles brought in contact are held together. However, it is unlikely that these forces alone will lead to spontaneous formation of agglomerates; extrinsic factors, such as mechanical stress, strain, vibration, humidity and temperature may also play major roles in the API auto-agglomeration process [18,20–23].

Fundamentally, auto-agglomeration of an API manifests itself when attractive interparticle forces/energies prevail over disruptive forces/energies [24–26]. For instance, vertical mechanical vibration has been utilized to produce agglomerates of fine powders, for which the equilibrium size and inherent strength were found to be dependent on the strength of attractive interparticle forces and mechanical vibration intensity [14,15,27]. A snow-balling process was proposed to explain the mechanism of agglomerate growth induced by mechanical vibration in which small particles stick onto the surface of larger particles and/or of already formed agglomerates. Size and mass mismatch drive agglomeration due to the predominance of the cohesive energy of the bigger particles over the kinetic energy of the collision of the small particle [15]. Other possible modes of auto-agglomeration include densification of soft agglomerates, fusion of the primary particles, their sintering as well as accumulation of tribo-electric charges within the bulk powder [1,17,18,23,28].

The engineering of a given particle of the API is often carried out using crystallisation procedure [29–31]. For instance, the surface chemistry of the API, which impacts physico-chemical and biopharmaceutical properties of an API as well as its manufacturing and handling behaviour, may be controlled through altering the crystal morphology of the API particle that is defined by different proportions of different crystal facets [29]. Although there are numerous studies addressing the relationship between API crystal surface chemistry, powder properties and behaviour [13,32,33], the role of the particle morphology and surface properties on dry API auto-agglomeration has not been elucidated.

This work examines possible correlations between particle engineering, particle physicochemical properties and post-processing with dry API auto-agglomeration. The specific aim was to determine whether particle morphology and surface properties, i.e., crystal polarity, impact the tendency to undergo auto-agglomeration. Ibuprofen recrystallised in different solvents was used as the model API. Its auto-agglomeration tendency was tested using mechanical vibration that, to some extent, could correspond to drug handling conditions. Ibuprofen samples were characterized to define their molecular structure (Fourier Transform Infrared, FTIR), crystallinity (Powder X-ray Diffraction, PXRD), particle size (optical and laser diffraction), morphology (scanning electron and optical microscopies), and propensity to acquire tribo-electric charge. The latter is one of the crucial phenomena taking place during powder mechanical vibration, thus, potentially affecting powder auto-agglomeration process. In addition, approaches to characterise the strength of agglomerates/agglomerated powder were investigated.

2. Materials and methods

(RS)-ibuprofen (50 μm grade) was supplied by AstraZeneca Ltd. and was recrystallised in hexane (99%, Fisher Scientific, UK), acetonitrile (≥99.5%, Sigma-Aldrich, UK), ethanol (≥ 99.8%, VWR Chemicals, UK), and methanol (≥99.8%, Fisher Scientific, UK).

Based on ibuprofen solubility data [29,31], supersaturated ibuprofen solutions were prepared with the following concentrations: hexane 1.1 g/ml, acetonitrile 1.42 g/ml, ethanol 1.5 g/ml, and methanol 2.1 g/ml. These solutions were heated to 60 °C and then cooled linearly at a rate of 1 °C/min in a jacketed Optimax reactor. The solutions were seeded with 1% of starting material prior to nucleation and then further cooled linearly at the same rate to 1 °C. Crystals were separated from the solution by filtering through general-purpose laboratory filter paper (Whatman, UK). The resulting wet solid powder was dried in an oven at 50 °C for 24 h. Prior to further characterisation, each recrystallised batch was sieved through a stainless-steel sieve with a mesh of 150 μm using a sieve shaker (EML, Haver & Boecker, Germany), operating with an amplitude of 0.5 mm, over intervals of 10 s for 10 min.

To induce auto-agglomeration by mechanical vibration, 1 g of ibuprofen powder was filled into an acrylic box (60 mm × 60 mm × 60 mm) mounted in an electrodynamic shaker (Model K2007E01, the Modal Shop Inc., Ohia, USA). Vibration was sustained at a frequency of 110 Hz and an amplitude of 3 mm for 20 min to ensure powder vibrates throughout the experiment.

Attenuated total reflectance-Fourier transform infrared (ATR-FTIR) spectroscopy was performed using the Thermo Science IS 10 fitted with a Smart iTR ATR module and a diamond crystal. Pressure in the order of 10,000 psi was applied with a high-pressure clamp to the samples and each spectrum was acquired as an average of 32 interferograms. Qualitative analysis was carried across the entire 650–4000 cm^{-1} range. Background absorption was subtracted from the sample runs.

Powder X-ray diffraction (PXRD) was performed with a Bruker D8 diffractometer, in Bragg-Brentano geometry with a standard Bruker powder diffraction holder. Cu K_α radiation ($\lambda = 0.154$ nm) was generated from an X-ray bremsstrahlung tube operating with 40 kV acceleration voltage and 40 mA current. 1° fixed divergence slits were applied to the incident X-ray beam. Scans were acquired over a 2θ range of 10° to 50°, in steps of 0.035°. For each ibuprofen batch, relevant percentages of (011) and (100) crystal facets were calculated by comparing their areas under the curve (AUC) to AUC of all the peaks present in PXRD data.

A Carl Zeiss EVO MA15 SEM instrument was used to perform scanning electron microscopy (SEM) to qualitatively assess particle size, shape and surface topography. The samples were placed on the carbon tabs placed on SEM metal pin stubs, then sputter-coated with a thin (5 nm) layer of iridium in preparation for SEM analysis to minimize

charging. A voltage of 20 kV and working distance of 10 mm were used.

The particle size and shape of as-recrystalised and mechanically vibrated ibuprofen samples were determined using a Morphologi G3-S (Malvern Instruments Ltd.; Malvern, UK) apparatus, as it provides access to particle shape characteristics as well. A small volume (11 mm^3) of dry ibuprofen powder was placed into the sample dispersion unit. The powder was dispersed with 0.5 bar 'pulse' of nitrogen and allowed to settle over 1 min on the G3 stage glass. A 5× lens was used (measuring range 6.5–420 μm) to acquire images of the dispersed sample. Around 40,000 particles were imaged for each run. Once scanned, particle parameters were determined with the G3 software with the size reported using the circle equivalent diameter (CE diameter) and the shape reported using the aspect ratio [34]. The width of the size distributions was evaluated by calculating the span using the following formula: span = $(D_{90}-D_{10}) / D_{50}$ [35].

The strength of auto-agglomerates was characterized with an Aero S dry powder standard disperser unit (this has a straight-through connection to the measurement cell) for the Malvern Mastersizer 3000. Particle size distribution measurements were performed for 8 ibuprofen samples, average data of which were then used for the particle strength studies. Each batch was dispersed in air at pressures of 0.1, 2, 3, and 4 bar (3 repeats at each bar pressure). Backgrounds were acquired over 10 s, followed by measurements over 10 s at a feed rate of 50% and obscuration above 0.5%.

Powder tribo-electrification during dispersion was measured using a previously described method [36] placing the dispersion unit of the Malvern Morphologi G3 onto a Faraday cup connected to an electrometer. All the components of the dispersion setup used for this study were made of stainless steel. After recrystallization and drying, samples were sieved and left in glass vials for several days before the test. 3 mm^3 bulk volume from each sample were weighted and then dispersed at 0.5 bar dispersion pressure and 20 ms pulse time. The tests were conducted at the temperature and relative humidity of 22–23 °C and 41–43%, respectively and repeated at least ten times to make sure of a reproducible value. Then the results for average charge to mass and to surface area ratios were studied. The surface area was calculated using the Morphologi G3 data collected at 0.5 bar dispersion pressure.

For the analysis, a work function of 4.77 eV [37] was assumed for ibuprofen and 4.3 eV [38] for stainless-steel.

3. Results and discussions

The scientific primary literature is rich in papers regarding crystallisation solvent effects on ibuprofen crystal morphology and consequential differences in its crystal surface properties and powder behaviour [29–33,39–41]. Decreasing solvent polarity decreases regularity of the crystal morphology from rectangular prism-like to needle-like as demonstrated in Fig. 1. Changes in crystal morphology imply a change in the proportions of the crystal facets. Literature indicates that there are three main facets of ibuprofen: (100), (011) and (002) [29,31,41]. The dominant (100) facet contains aliphatic chains at its surface, whereas the other two of the main three facets of the ibuprofen crystal have carboxylic acid groups exposed at their surfaces. The polarity of the (011) and (002) facets is greater than that of (100) due to the nature of the functional groups exposed at their surfaces. Therefore, the overall polarity of the ibuprofen crystal surface and specific surface energy go down as the relative presence of (011) and (002) facets decrease.

3.1. Recrystallised materials

SEM images of the recrystallised ibuprofen samples *(*Fig. 2*)* prior to mechanical vibration show how crystal morphology varies as a function of the solvent medium used for recrystallisation. As expected from previous studies [29,32,40], the morphology changes from rectangular prism-like to needle-like as the polarity of the solvent decreased (methanol > ethanol > acetonitrile > hexane), i.e., higher solvent polarity favours higher aspect ratios.

The characteristic particle size distribution (PSD) parameters for the recrystallised materials, measured using morphologi G3, are presented in Table 1, along with the representative 2D images of the particles acquired by static image analysis *(*Fig. 3*)*. The d_{50} and d_{90} aspect ratio values *(*Table 1*)* decrease as a function of solvent polarity, in the following order: methanol > ethanol > acetonitrile > hexane. The cumulative number- and volume-based particle size distributions *(*Fig. 4*)* for the recrystallised ibuprofen samples indicate that, recrystallisation from hexane results in the highest proportion of fines (< 10 μm) and the lowest proportion of coarse (> 50 μm) particles. All particle size distributions indicate the presence of particles larger than 150 μm which is larger than the sieve mesh size of 150 μm. This is expected as larger particles can pass through the mesh when orientated with their principal axis perpendicular to the mesh plane.

FTIR spectroscopy and PXRD were also performed on the recrystallised ibuprofen samples to determine the molecular structure and the polymorphic form of the ibuprofen, respectively. FTIR analysis did not indicate differences between the ibuprofen samples *(Fig. S1)*. This is expected as this technique is relatively insensitive to particle morphological variations.

PXRD patterns of four samples *(*Fig. 5*)* reveal the alignment of the Braggs peaks over the whole scanning range. The measured patterns correspond to ICDD database data for ibuprofen single crystal form I confirming recrystallisation, independently of solvent used, did not result in the form change from (*RS*)-ibuprofen form I, since the only other form (form II) reported in the literature was produced by

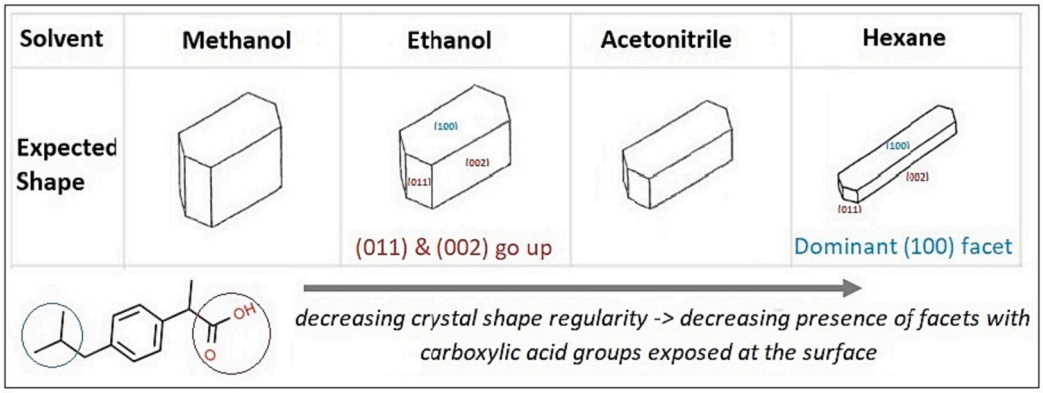

Fig. 1. Schematics showing ibuprofen molecule and the effect of crystallisation solvents on ibuprofen crystal morphology: (100) facet contains aliphatic chains, whereas (011) and (002) facets have carboxylic acid groups exposed at their surfaces. The greater proportion of (011) and (002) facets is believed to be associated with higher polarity of the crystal and higher specific surface energy.

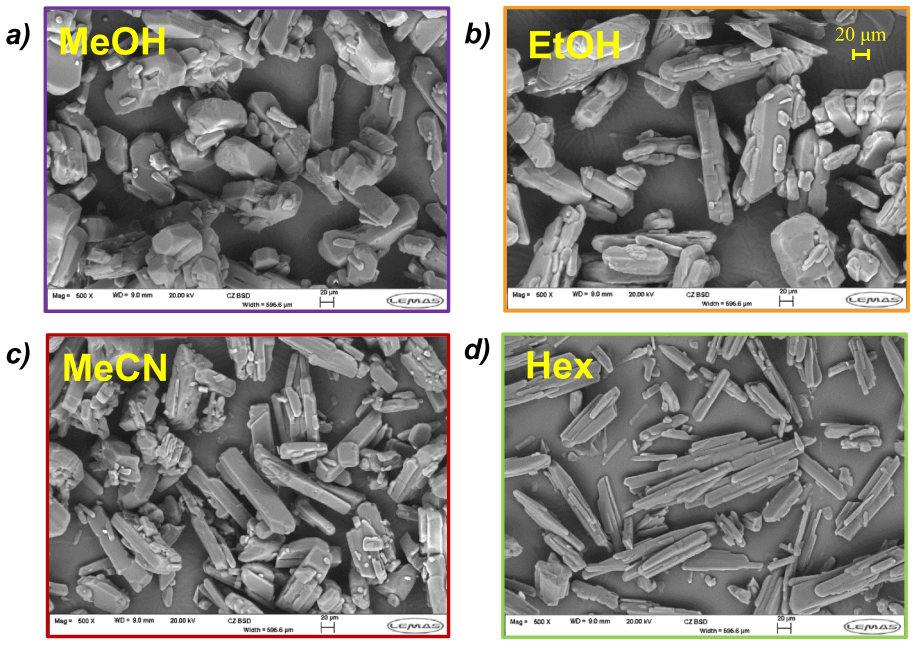

Fig. 2. SEM images showing changes in particle morphology of ibuprofen particles recrystallised from: a) methanol (MeOH) b) ethanol (EtOH) c) acetonitrile (MeCN) d) hexane (Hex). Images captured using 500× magnification.

Table 1
Summary of the volume-based size profiles, including span and aspect ratio values, of as-recrystallised and after mechanical vibration ibuprofen samples, data collected using Morphologi G3.

Recrystallisation solvent	Volume-based particle size (µm)												Auto-agglomeration induced by mechanical vibration
	As-recrystallised ibuprofen						As-recrystallised ibuprofen after mechanical vibration						
	D10	*D50*	*Aspect ratio (d50)*	*D90*	*Aspect ratio (d90)*	*Span*	*D10*	*D50*	*Aspect ratio (d50)*	*D90*	*Aspect ratio (d90)*	*Span*	
methanol	67	121	0.54	192	0.60	1.03	76	138	0.57	198	0.57	0.86	Weak
ethanol	68	129	0.51	202	0.58	1.05	120	195	0.60	326	0.61	1.06	Strong
acetonitrile	52	110	0.49	175	0.54	1.12	87	158	0.55	240	0.62	0.97	Strong
hexane	31	70	0.39	136	0.45	1.5	26	60	0.47	138	0.53	1.87	Absent

annealing [42,43]. Observed differences in signal intensities may be due to a number of factors, such as variations in surface texture of the sample and/or the preferred orientation of the particles of distinct morphology [40,44].

Importantly, PXRD data was used to evaluate the differences in proportion of (011) and (100) crystal facets as a function of the crystallisation solvent used. The (011) facet was chosen for this analysis as it appears as a distinct single Braggs peak and is one of the main facets containing carboxylic acid groups exposed at its surface. Relevant percentages of the relatively polar (011) facet for each ibuprofen sample can be found in Table 2: its proportion decreases from 0.94% to 0.78% as the polarity of the crystallisation solvent decreased from methanol to hexane, in line with literature findings suggesting crystallisation of ibuprofen in polar solvents results in greater proportion of polar facets [31,39]. The percentage values are relatively small reflecting the fact that PXRD data captures all existing facets of ibuprofen crystal, i.e., there might be numerous facets beyond the three main ones discussed in this paper and in the literature [32,33,41]. Nevertheless, changes in

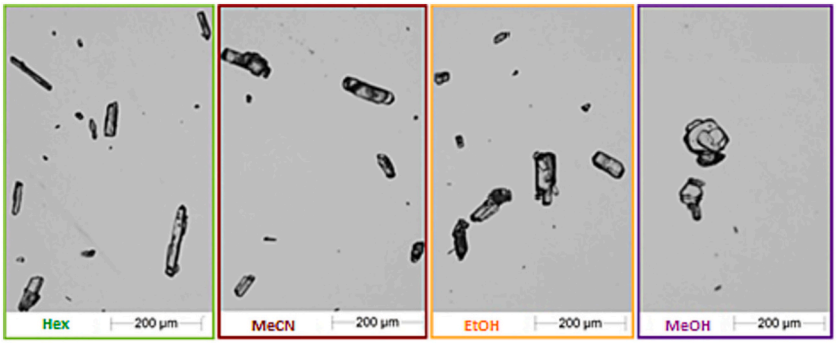

Fig. 3. 2D images of ibuprofen samples showing differences in particle morphology as a function of solvent used: hexane (Hex), acetonitrile (MeCN), Ethanol (EtOH), and methanol (MeOH). The scale bar is 200 µm.

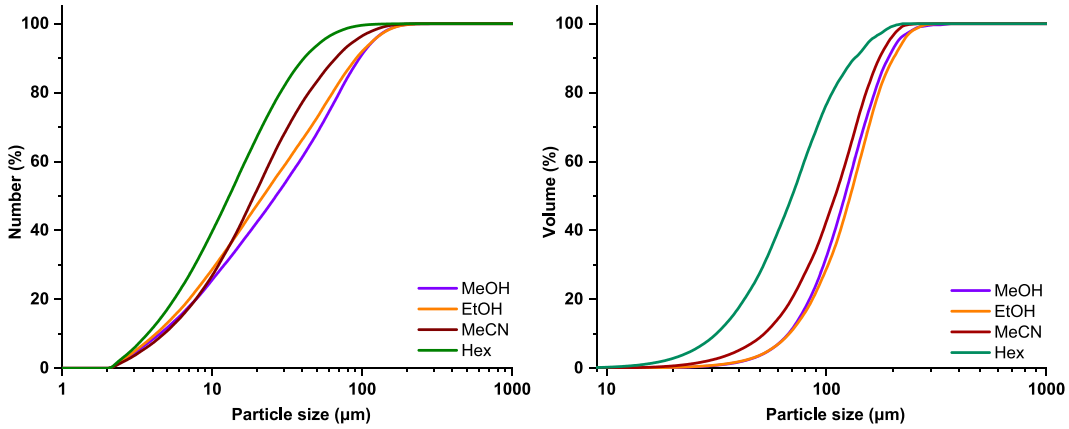

Fig. 4. Number-based and volume-based cumulative particle size distributions of ibuprofen samples recrystallised from methanol (MeOH), ethanol (EtOH), acetonitrile (MeCN), hexane (Hex), Morphologi G3.

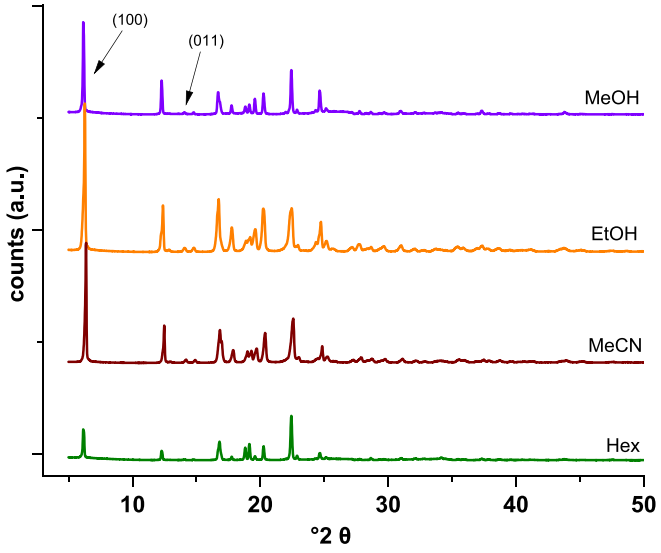

Fig. 5. PXRD data of ibuprofen samples recrystallised from methanol (MeOH), ethanol (EtOH), acetonitrile (MeCN), hexane (Hex). Intensities normalized to the peak at 22.5 deg.

presence of (011) facet suggest crystal surface polarity gets lower in ibuprofen samples in the following order: methanol > ethanol > acetonitrile > hexane, corresponding with variations in particle morphology (Fig. 2, Table 1). The contribution percentages of the (100) facet (the non-polar facet), are also included in the Table 2, where a slightly greater presence of the (100) facet in the MeOH compared to the other batches could be linked to its aspect ratio values for both d_{50} and d_{90}-sized particles which are the highest amongst the as-recrystallised batches (Table 1).

3.2. Materials after mechanical vibration

After mechanical vibration, auto-agglomerates were observed in the ibuprofen samples recrystallised from ethanol and from acetonitrile, as seen in the SEM images in Fig. 6.

The cumulative volume distributions of mechanically vibrated samples together with the as-recrystallised samples, for an ease of comparison, are shown in Fig. 7 *and* Table 1. According to PSD data, and in line with the SEM findings, mechanical vibration caused enlargement in particle size in the case of ibuprofen recrystallised from ethanol and from acetonitrile to the following extent: 45% of the EtOH(v) and 41% of the MeCN(v) particles were found to be above d_{90} of the original batches of EtOH and MeCN, respectively ((v) stands for "vibrated"). Weak auto-agglomeration, that is slight increase in d_{10}, d_{50}, and d_{90} values, was observed in the batch recrystallised from methanol. In contrast, the volume-based size of the batch recrystallised from hexane slightly decreased upon mechanical vibration. This may be due to the needle-like particle morphology of the batch recrystallised from hexane that, in general, is prone to breakage more than the less irregular shaped particles [32]. Also, the aspect ratio value of d_{90} decreased in MeOH(v) compared to MeOH (Table 1) which may be a sign of the breakage of the pre-existing in as-recrystallised MeOH batch thick d_{90} particles/agglomerates (Fig. 2 versus Fig. 6) and/or of the newly formed agglomerates at the vibration intensities chosen to induce auto-agglomeration.

The size measurements of as-recrystallised and mechanically vibrated ibuprofen batches were also collected using a Mastersizer 3000 (dry method). These results can be found in the supplementary information section in the form of *Table S1* containing PSD values. The Morphologi G3 and Mastersizer PSD data are not aligned due to the inherent differences between the two methods, such as the amount of material analysed per test, the different size limits, how the

Table 2
Relative percentages of (100) and (011) facets (based on PXRD data) for as recrystallised and after mechanical vibration ibuprofen samples, and tribo-electric surface charge densities for as-recrystallised ibuprofen, recrystallised from methanol (MeOH), ethanol (EtOH), acetonitrile (MeCN), hexane (Hex).

Recrystallisation solvent	PXRD				Tribo-charging (μC/m^2) of as-recrystallised ibuprofen	Auto-agglomeration induced by mechanical vibration
	As-recrystallised ibuprofen		Ibuprofen after mechanical vibration			
	%(100) facet	%(011) facet	%(100) facet	%(011) facet		
Methanol	13.66	0.94	10.04	0.98	−2.62	Weak
Ethanol	12.86	0.92	17.48	0.94	−1.96	Strong
Acetonitrile	12.44	0.90	14.54	0.92	−2.02	Strong
Hexane	11.40	0.78	6.55	1.01	−3.50	Absent

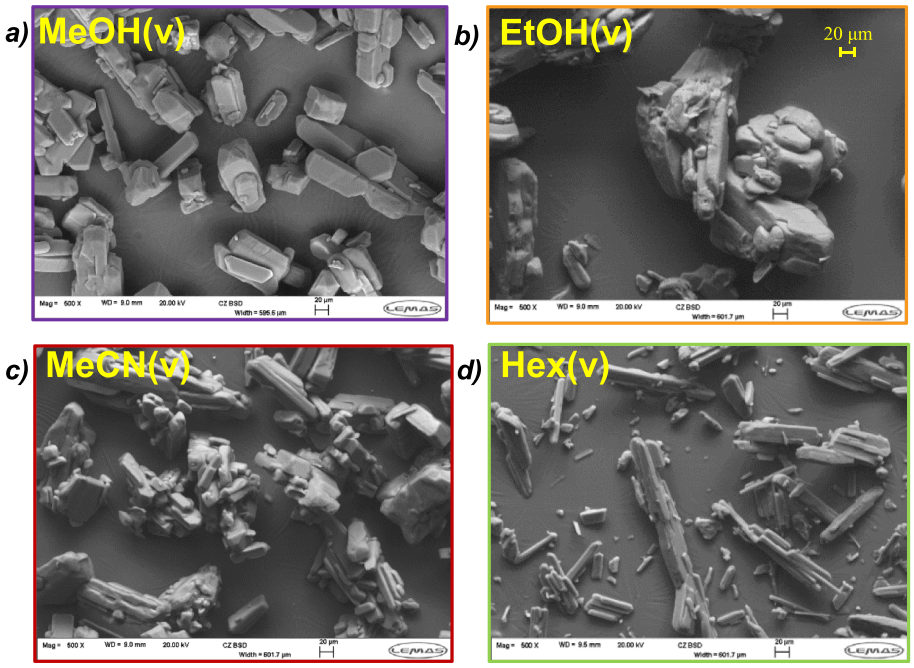

Fig. 6. SEM images of recrystallised ibuprofen samples after mechanical vibration for 20 min at 110 Hz frequency and 3 mm amplitude, recrystallised in: a) methanol (MeOH(v)) b) ethanol (EtOH(v)) c) acetonitrile (MeCN(v)) d) hexane (Hex(v)). Images captured using 500× magnification.

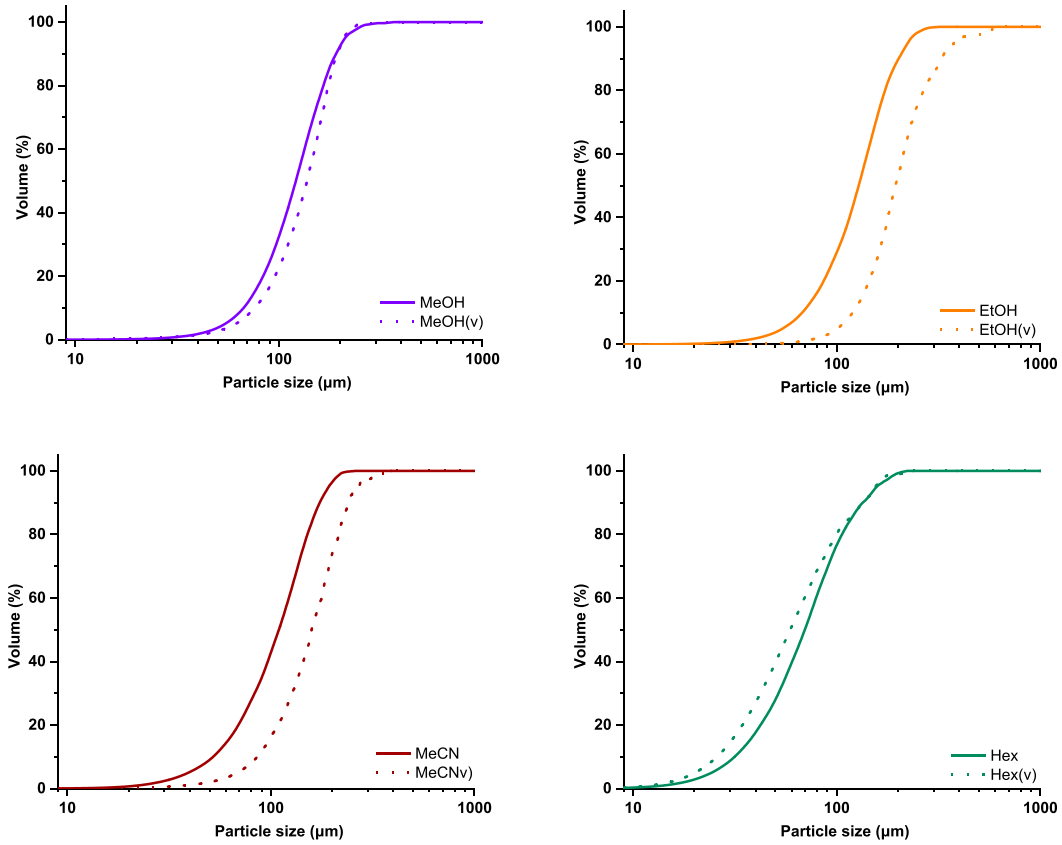

Fig. 7. Volume-based cumulative PSD spectra of as recrystallised and after mechanical vibration ibuprofen samples, recrystallised from methanol (MeOH), ethanol (EtOH), acetonitrile (MeCN), hexane (Hex), "(v)" in the name stands for "after mechanical vibration", Morphologi G3.

measurements are collected, etc. However, they show close agreement in batch size variations (in as-recrystallised batch-to-batch as well as in as-recrystallised batch-to-mechanically vibrated batch) confirming a strong presence of auto-agglomerates in EtOH(v) and MeCN(v) samples.

PXRD data for ibuprofen samples that were mechanically vibrated reveals that no major changes in peak positions occurred, i.e., mechanical vibration did not result in its crystallinity and/or crystal form change (supplementary information *Fig. S2*). The effect of mechanical

vibration on the relative percentages of (011) and (100) facets was also studied. As presented in Table 2, the percentage values indicate an increase in the presence of the relatively polar (011) facet in all samples but more so in the case of MeOH(v) and Hex(v) batches being vibrated, which links with the decrease in d90 aspect ratio value of MeOH after vibration and breakage of Hex particles. In addition, the (100) facet relative percentages in mechanically vibrated batches decrease as follows: EtOH>MeCN >MeOH>Hex linearly correlating with the auto-agglomeration trend.

3.3. Strength of auto-agglomerates

Various approaches were tried in the past to assess hardness of agglomeration, including sieving [45], and compression tests [46], though both were not plausible for this study as sieving requires large amounts of material, whereas, compression tests return high fracture force standard deviation values. It was necessary to develop a comparative approach to assess the strength of the primary particles and of the agglomerates to be able to establish the magnitude of the problem, hence, to establish if auto-agglomeration detected in after mechanical vibration ibuprofen samples could possibly impact the drug manufacturing process and/or drug performance. Ultimately, dry laser diffraction (Mastersizer 3000) pressure ladder approach was chosen allowing to measure the strength of all particles in the bulk (unlike, for instance, compression tests) while utilizing moderate amount of material per test. On the basis of the pressure ladder approach, the following two distinct analysis methods were developed: 1) dispersion index (DI), inspired by the work of [47]; 2) Agglomerate Strength Index (ASI). Although the same approach to testing agglomerates strength based on the dispersion pressure ladder could be potentially tried out using Morphologi G3 instrument, for this study we concentrated only on laser diffraction data after taking into consideration the facts that Mastersizer 3000 (dry method) is a faster technique (time required per test), it measures more particles per test and particle morphology data was not planned to be used for the agglomerate strength calculations.

The DI method facilitated a quick and efficient analysis of the effect of auto-agglomeration on the bulk powder dispersion behaviour, where volume-based PSD data collected at 0.1 and 2 bar pressures were used. The overlapping area under the curve (AUC) from the two distributions was used to define the DI of a sample *(*Eq. (2)*)*. An example illustrating the overlapping AUC is depicted in the Fig. 8 and *Fig. S3* in Supplementary Information, which could be estimated using the trapezium rule or by the following equation:

$$AUC = \int_{d_0}^{IP} f_{0.1}\,dPS + \int_{IP}^{d_f} f_2\,dPS \quad (1)$$

where $f_{0.1}$ and f_2 represent the distributions for the powder dispersed at 0.1 and 2 bar pressures respectively, d_0 and d_f are the initial and final points of $f_{0.1}$ and f_2 distributions, respectively. *IP* is the intersection point of the two distributions and *PS* is the particle size in μm.

$$DI = AUC_r / AUC_v \quad (2)$$

where subscript *r* represents recrystallised samples, and subscript *v* – sample after mechanical vibration.

A DI of 1 means mechanically vibrated powder will disperse similar to as-recrystallised powder, hence little or no strong auto-agglomeration could have occurred after the vibration. A DI of lower than 1 for the mechanically vibrated powder indicates to its stronger constituents than as-recrystallised powder. A DI of bigger than 1 could indicate to particle breakage after the mechanical vibration.

The DI profiles of eight ibuprofen samples are summarised in Table 3 revealing that, indeed, the two batches that did strongly agglomerate upon mechanical vibration had the lowest DI values, hence, the dispersion extent of the powder decreases as the auto-agglomeration tendency of it increases as follows: Hex(v) > MeOH(v) > MeCN(v) > EtOH(v), standard deviations for DI are not included as the highest value was 0.007 for EtOH batch. The DI of 1.1 for the Hex(v) batch indicates that mechanical vibration induced breakage of these needle-like particles.

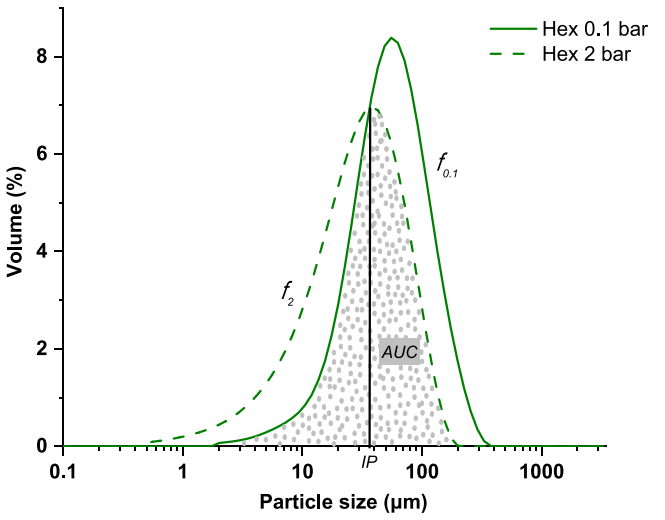

Fig. 8. Volume-based particle size distribution of ibuprofen recrystallised from hexane (Hex) obtained using Mastersizer 3000 (dry method) at 0.1 and 2 bar pressures, the dotted area is the area under the curve (AUC) of the two distributions.

Table 3
Dispersion Index and Agglomerate Strength Index profiles of as recrystallised and after mechanical vibration ibuprofen samples, recrystallised from methanol (MeOH), ethanol (EtOH), acetonitrile (MeCN), hexane (Hex), "(v)" in the name stands for "after mechanical vibration"; standard deviations (STD) for ASI are shown in brackets.

Sample	Dispersion Index (DI)	Agglomerate Strength Index (ASI)			Auto-agglomeration induced by mechanical vibration
		D10	D50	D90	
EtOH	0.93	0.45 (0.02)	0.47 (0.04)	0.51 (0.06)	Strong
EtOH (v)		0.45 (0.04)	0.45 (0.01)	**0.59** (0.05)	
MeCN	0.95	0.43 (0.04)	0.46 (0.05)	0.52 (0.03)	Strong
MeCN (v)		0.40 (0.02)	0.46 (0.03)	**0.56** (0.03)	
MeOH	0.99	0.53 (0.02)	0.48 (0.03)	0.53 (0.01)	Weak
MeOH (v)		0.47 (0.00)	0.43 (0.02)	**0.51** (0.02)	
Hex	1.1	0.24 (0.00)	0.47 (0.04)	0.48 (0.02)	None
Hex(v)		0.23 (0.02)	0.44 (0.07)	**0.48** (0.01)	

A second method, the ASI, was developed to investigate the strength of the d_{10}, d_{50}, and d_{90} individually and to determine which size fraction affects the DI of the vibrated powder the most and, possibly, get insights into the auto-agglomeration mode. The PSD data collected at 4 different dispersion pressures were fitted to asymptotic exponential function ($y = a\text{-}b*c^x$), and the term *c* related to the rate of the decay in size was defined as the Agglomerate Strength Index (ASI): the higher the index the stronger the agglomerates. The example of the gathered data and the fitting are shown in Fig. 9, and the ASI values for all 8 ibuprofen batches are provided in the Table 3. In Fig. 10 the ASI versus particle size for different batches (as recrystallised and vibrated) is plotted.

Firstly, from the data presented in Table 3, the ASI values showed

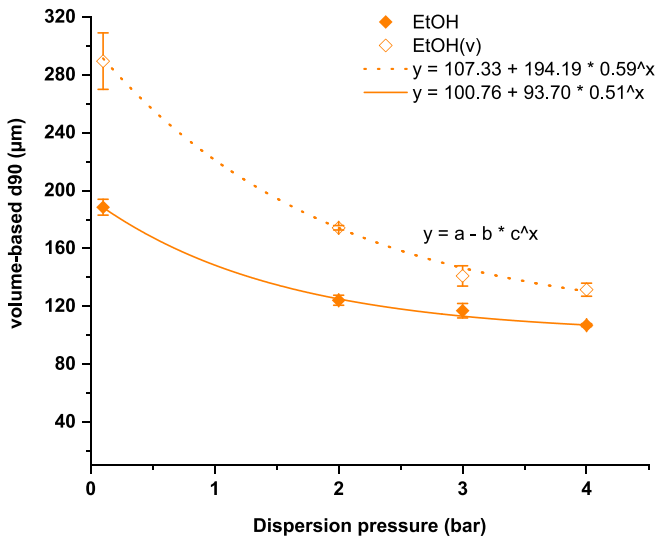

Fig. 9. Fitting the pressure ladder data obtained using Mastersizer 3000 (dry method): the rate of decay in size was defined as Agglomerate Strength Index (ASI), examples are based on the d_{90} values of ibuprofen recrystallised in ethanol (EtOH and EtOH(v)), "(v)" in the name stands for "after mechanical vibration").

that generally the strength index of d_{90} particles is higher than of d_{50}, presumably due to the larger aspect ratios of the bigger particles. Nevertheless, no relationship between strength index of d_{10}, d_{50}, d_{90} particles across the as-recrystallised batches (before vibration) and the tendency of these batches to auto-agglomerate was found.

Observation from the Fig. 10, in line with previously discussed PSD data, is that all EtOH and MeCN size fractions significantly enlarged upon mechanical vibration suggesting that the auto-agglomeration mode, in this case, involves sticking of the smaller particles onto the surface of the larger ones. Normally, depending on the ratio of cohesion over collision energy, the two like-sized large particles would rebound or stick together but relatively loosely, while sticking of unlike-sized particles could lead to a formation of auto-agglomerates with inherent strength [14,15,24,25]. Indeed, out of all particle size fractions of the EtOH(v) and MeCN(v) batches that enlarged upon mechanical vibration, it is only their d_{90}-sized particles/agglomerates that got stronger according to ASI calculations (Table 3), presumably because large agglomerates would attract smaller particles and become more consolidated during vibration. Moreover, the increase in d_{90} strength correlates with ibuprofen auto-agglomeration tendency trend as follows: d_{90} strength indices of EtOH(v) and of MeCN(v) are 0.59 and 0.56, respectively, whereas d_{90} strength indices of MeOH(v) and Hex(v) are 0.51 and 0.48, respectively, indicating that the strength of the d_{90} size fraction could be playing the major role in the strength of the vibrated powder affecting the DI the most.

Finally, by combining the SEM observations of EtOH(v) and MeCN (v) samples (Fig. 6), which suggest that the particles are tightly bound to

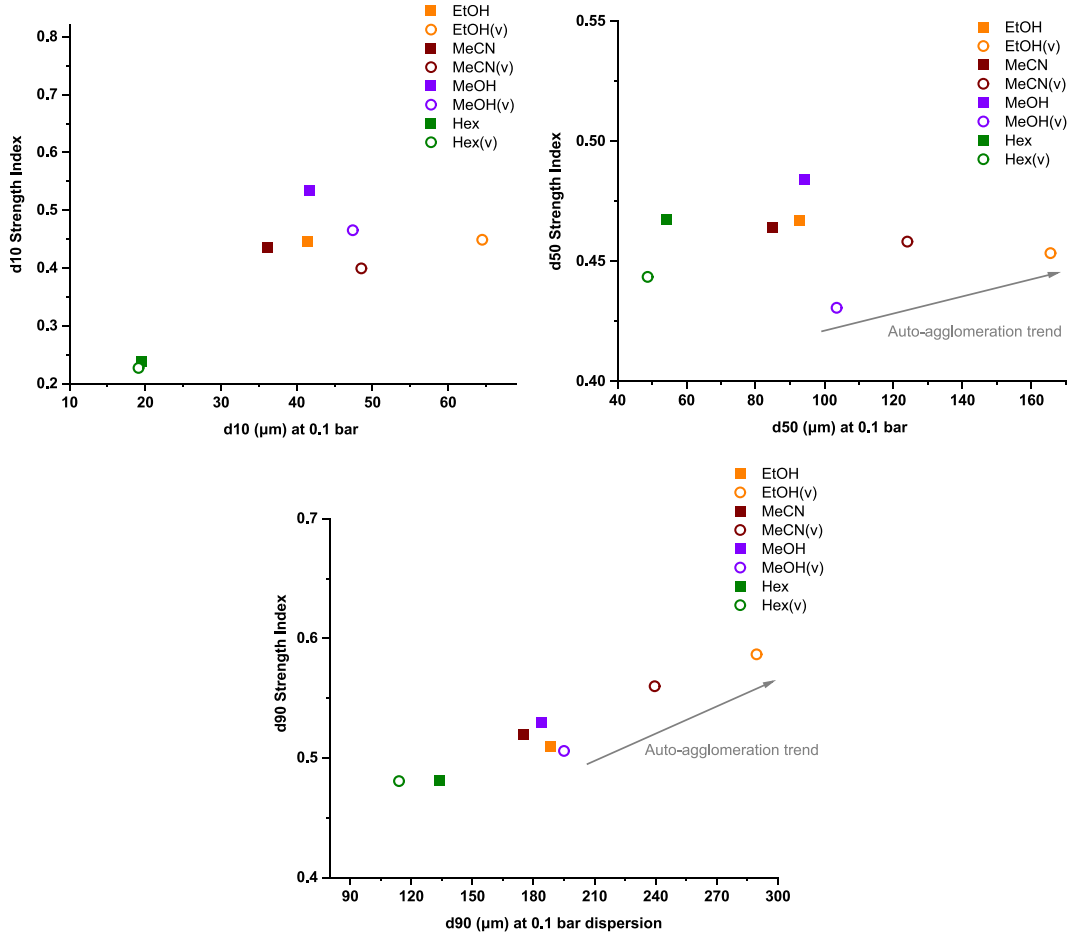

Fig. 10. Strength Index versus particles size of samples recrystallised from methanol (MeOH), ethanol (EtOH), acetonitrile (MeCN), hexane (Hex), "(v)" in the name stands for "after mechanical vibration". Strength Index was calculated using dry Mastersizer 300 pressure ladder method, size values collected at 0.1 bar dispersion pressure were used.

each other, and their relatively large d_{90} strength values, it can be postulated that the obtained EtOH(v) and MeCN(v) auto-agglomerates could be due to the fusion of the mismatched in size original particles, although further investigations of the internal structure of these auto-agglomerates would be required to verify this statement as well as to explore if densification of the agglomerates took place during mechanical vibration.

Since mechanical vibration induce strong auto-agglomeration only in two out four recrystallised ibuprofen batches, further work is focused on investigation of triboelectrification propensities of these samples – the phenomenon that, amongst other factors, relates to the surface chemistry of the particle as well as powder processing/handling.

3.4. Tribo-charging

The mechanical vibration method, used in this study to induce auto-agglomeration of ibuprofen, involves frequent particle-particle and particle-vibration box walls contacts (either by impact, shear or friction) that could result in electrostatic charging of the powder known as triboelectrification [48]. As reported in the literature, triboelectrification mechanisms include electron (the main route in the case of pharmaceutical powders), ion and material transfer arising due to the difference in the work function of the materials in contact when electrons move from the material with lower work function to that with a higher value [49]; but triboelectrification may also be affected by particle size, surface chemistry/composition, environmental factors, etc. [28,50,51].

Ibuprofen is an overall relatively non-polar molecule consisting of a large non-polar body and a small polar head suggesting it is an insulating material that is prone to acquire triboelectric charge. Its charging tendencies against various materials were reported previously [37,52]. However, the impact of recrystallisation solvent, hence, ibuprofen surface composition on its tribo-charging propensity reported here for the first time. Since the polar interactions are associated with electron transfer [28,53,54], it was hypothesised that the tribo-charging magnitude might be affected by the ibuprofen particle morphology as the more regular (rectangular prism-like) shaped particles and particles that are prone to breakage, in accordance with the PXRD findings discussed in Section 3.1 and 3.2 *(*Table 2*)*, have greater proportion of relatively polar crystal facets with carboxylic acid groups exposed at their surface.

As anticipated from the work function values of the materials in contact, the charge-per-mass data shown in Fig. 11 revealed that all ibuprofen batches charged negatively upon the contact with stainless steel during its dispersion using the tribo-charging rig. The magnitude of the charge-per-mass ratios reflects the differences in size across the batches: the ibuprofen recrystallised from hexane (Hex), the batch with the smallest PSD values, was found to charge the most compared to other ibuprofen samples. This is due to the increase in the total surface area of the material in a measured volume [48]. As the tribo-charging dispersion system is the same as used in the Morphologi G3 size measurements, it was sensible to use the surface area obtained from Morphologi G3 in the calculation of charge per surface area, namely tribo-electric surface charge density. It should be noted that the same dispersion pressure (0.5 bar) has been used in tribo-charging experiments as the Morphologi G3 for the surface area measurement. Normalized by surface area tribo-charging data, shown in Fig. 12 *and* Table 2*,* indicated that the EtOH and MeCN batches acquired smaller tribo-electric charges compared to MeOH and Hex batches.

Two major observations can be made based on the results mentioned above. Firstly, the acquired triboelectric charge inversely correlates with auto-agglomeration tendencies of ibuprofen recrystallised from solvents of diverse polarities as follows: the lower the magnitude of the gained charge, the greater the tendency to auto-agglomerate *(*Table 2*)*.

The second significant observation arising from the tribo-electrification experiments is that no direct correlation between morphology as well as surface polarity of the as-recrystallised ibuprofen particles and their triboelectrification was found, since the particles with most extreme aspect ratios associated with the highest and lowest surface polarities (MeOH and Hex, respectively), gained greater tribo-electric charge compared to the EtOH and MeCN particles. A higher electrostatic charge for rectangular prism-like MeOH particles is expected since they have the highest relative percentage of (011) facet and surface polarity. However, Hex particles were not expected to gain the highest electrostatic charge since they have the lowest surface polarity. In the particle size and shape analysis section we established that particles recrystallised from hexane (needle-like particles) are prone to breakage. According to previous studies [32], the breakage mechanism of needle-like particles is of a random nature occurring by attrition, as opposed to the breakage through slip plane. The attrition of the Hex particles increases the relative surface area of the polar facets in the sample *(*Table 2*)*, i.e. (011) and (002) facets that contain carboxylic acid groups at their surfaces. This is presumably the main reason that Hex particles gained higher electrostatic charge, despite their inherently

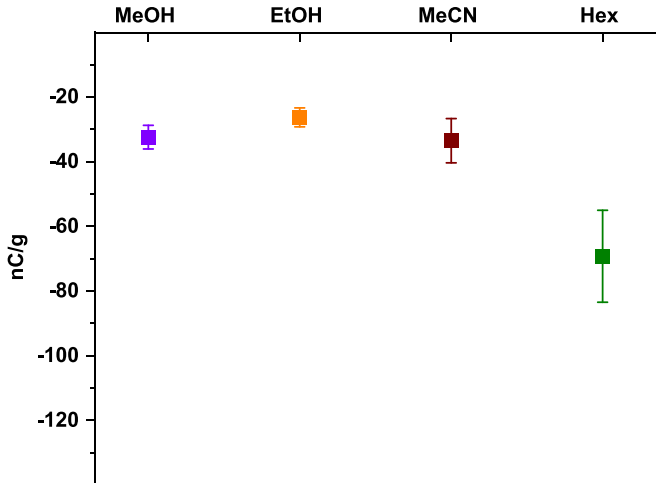

Fig. 11. Charge-to-mass ratios for ibuprofen samples, recrystallised from methanol (MeOH), ethanol (EtOH), acetonitrile (MeCN), hexane (Hex), against stainless steel surface at 0.5 bar dispersion pressure. The data of samples after mechanical vibration can be seen in the Supplementary Information.

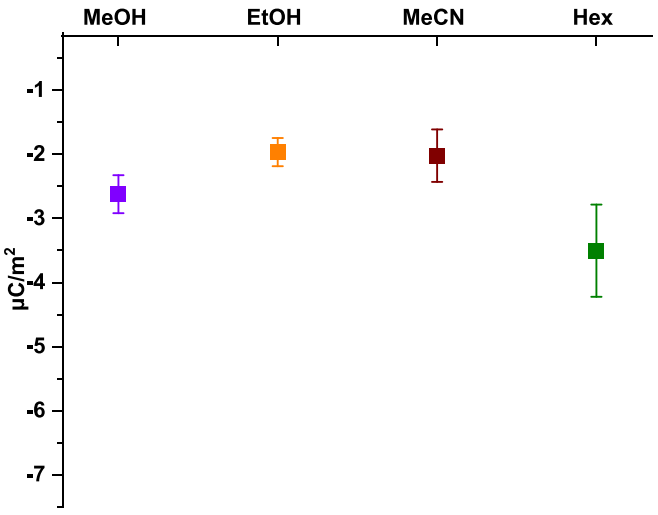

Fig. 12. Tribo-electric surface charge densities for ibuprofen samples, recrystallised from methanol (MeOH), ethanol (EtOH), acetonitrile (MeCN), hexane (Hex), against stainless steel surface at 0.5 bar dispersion pressure. Surface area calculated using morphologi G3 size data obtained at 0.5 dispersion pressure. The data of samples after mechanical vibration can be seen in the Supplementary Information.

lower surface polarity. The greater the polarity of the crystal, the greater the gained charge from the surface which it collides with. This allows a greater opposite charge attraction between the particles and the wall, while it reduces the probability of similarly charged particle attraction. Hence, at this level of examination the inverse correlation between triboelectrification and auto-agglomeration of ibuprofen can be rationalised by the reason that under the same mechanical vibration conditions the lower tribo-charging could favour greater particle-particle interactions and consequent formation of relatively weak agglomerates within the MeOH batch and larger and stronger agglomerates within the EtOH and MeCN batches.

Previously, the electrostatic charging of the APIs has been linked to their adhesion propensity, for instance, when the triboelectrification led to API sticking to the processing tooling [37,55], compromised powder flowability [56,57], and caused unwanted API-excipients adhesion [58]. In current investigation, during particles vibration a charge transfer can occur between particles and the box's walls resulting in the oppositely charged surfaces. However, ideally, tribo-charging of recrystallised ibuprofen against PMMA, the material of which the vibration box was made but was not available for the current triboelectrification study, should also be measured in future studies to confirm this statement.

Nevertheless, the tribo-electric surface charge densities for EtOH and MeCN samples are similar, despite the higher expected polarity of EtOH compared to MeCN samples. This should be further investigated using advanced particle surface analytical techniques, e.g. by X-ray photoelectron spectroscopy (XPS), to explore the surface chemistry of samples and possible surface anomalies, since the conventional analytical techniques used in this study may not be surface-sensitive enough.

4. Conclusions

In this study, we have investigated the vibrationally-induced auto-agglomeration of ibuprofen particles recrystallised in different solvents with different polarities. Two approaches were proposed to quantify the strength of agglomerates based on the analysis of size distributions during dry dispersion at different pressures, namely the dispersion and agglomerate strength indices. The dispersion index inversely correlates with the agglomerate strength index of d_{90} particles indicating to the auto-agglomeration tendencies of ibuprofen. We also established an inverse correlation between ibuprofen auto-agglomeration during mechanical vibration and the tendency of such particles to acquire triboelectric charges. Undesirable auto-agglomeration appears to be hindered by higher electrostatic charge due to higher surface polarity, which may be induced either by using the polar recrystallisation solvent (the highest aspect ratio particles) and/or by breakage of the particles during mechanical vibration resulting in more surfaces with polar functional groups being exposed. Higher surface polarity could favour electrostatic attraction to the walls of the vibration equipment, reducing the rate of cohesive interactions that lead to auto-agglomeration. Overall, we expect that this work stimulates further studies on the effect of particle surface chemistry on dry API auto-agglomeration, including on the correlation between powder auto-agglomeration and triboelectrification.

CRediT authorship contribution statement

Svetlana Bibiceva: Methodology, Investigation, Data curation, Conceptualization, Writing – original draft, Writing – review & editing. **Sven L.M. Schroeder:** Supervision, Writing – review & editing. **Ali Hassanpour:** Conceptualization, Supervision, Validation, Writing – review & editing.

Declaration of Competing Interest

The authors declare that they have no known competing financial interests or personal relationships that could have appeared to influence the work reported in this paper.

Data availability

Data will be made available on request.

Acknowledgment

This research was sponsored by the EPSRC Centre for Doctoral Training in Complex Particulate Products and Processes (EP/L015285/1) as part of a collaborative project with AstraZeneca Limited and Pfizer Limited, who we gratefully acknowledge. The authors would also like to thank Professor Mojtaba Ghadiri and his research group for facilitating access to the electrodynamic shaker apparatus and tribo-electerification device to study the auto-agglomeration behaviour. All data supporting this study are provided either in the results section of this paper or in the electronic supplementary information accompanying it.

Appendix A. Supplementary data

Supplementary data to this article can be found online at https://doi.org/10.1016/j.powtec.2023.119172.

References

[1] G. Nichols, et al., A review of the terms agglomerate and aggregate with a recommendation for nomenclature used in powder and particle characterization, J. Pharm. Sci. 91 (10) (2002) 2103–2109.
[2] E.D. Lachiver, et al., Agglomeration tendency in dry pharmaceutical granular systems, Eur. J. Pharm. Biopharm. 64 (2) (2006) 193–199.
[3] K. Kale, K. Hapgood, P. Stewart, Drug agglomeration and dissolution - what is the influence of powder mixing? Eur. J. Pharm. Biopharm. 72 (1) (2009) 156–164.
[4] M. Jaspers, et al., Impact of excipients on batch and continuous powder blending, Powder Technol. 384 (2021) 195–199.
[5] X. He, et al., Assessing powder segregation potential by near infrared (NIR) spectroscopy and correlating segregation tendency to tabletting performance, Powder Technol. 236 (2013) 85–99.
[6] D. Olusanmi, et al., A control strategy for bioavailability enhancement by size reduction: effect of micronization conditions on the bulk, surface and blending characteristics of an active pharmaceutical ingredient, Powder Technol. 258 (2014) 222–233.
[7] M. Scherholz, B. Wan, G. McGeorge, A rational analysis of uniformity risk for agglomerated drug substance using NIR chemical imaging, AAPS PharmSciTech 18 (2) (2017) 432–440.
[8] D. Ticehurst, et al., Characterisation of the influence of micronisation on the crystallinity and physical stability of revatropate hydrobromide, Int. J. Pharm. 193 (2) (2000) 247–259.
[9] P.J. Stewart, F.-Y. Zhao, Understanding agglomeration of indomethacin during the dissolution of micronised indomethacin mixtures through dissolution and de-agglomeration modeling approaches, Eur. J. Pharm. Biopharm. 59 (2) (2005) 315–323.
[10] USP, <905> Uniformity of dosage units. Stage 6 harmonization 2011, The United States Pharmacopeial Convention, 30 April 2022. Available from: https://www.usp.org/.
[11] M. Llusa, et al., Effect of high shear blending protocols and blender parameters on the degree of API agglomeration in solid formulations, Ind. Eng. Chem. Res. 48 (1) (2009) 93–101.
[12] J. Adamson, et al., Development of suitable plant-scale drying conditions that prevent API agglomeration and dehydration, Org. Process Res. Dev. 20 (1) (2016) 51–58.
[13] J.S. Stevens, et al., Detection of free base surface enrichment of a pharmaceutical salt by X-ray photoelectron spectroscopy (XPS), J. Pharm. Sci. 100 (3) (2011) 942–948.
[14] N. Ku, et al., Effect of mechanical vibration on the size and microstructure of titania granules produced by auto-granulation, Powder Technol. 286 (2015) 223–229.
[15] N. Ku, et al., Auto-granulation of Fine Cohesive Powder by Mechanical Vibration, Proc. Eng. 102 (2015) 72–80.
[16] M. Leaper, E. Fisk, R. Browne, Feasibility study to investigate caking in washing powder formulations using a Freeman FT4 powder rheometer, Part. Sci. Technol. 37 (8) (2019) 1005–1010.
[17] J.J. Fitzpatrick, et al., Comparing the caking behaviours of skim milk powder, amorphous maltodextrin and crystalline common salt, Powder Technol. 204 (1) (2010) 131–137.
[18] C.I. Haider, et al., Unwanted agglomeration of industrial amorphous food powder from a particle perspective, Chem. Eng. Res. Des. 132 (2018) 1160–1169.

[19] M.F. Saleh, et al., Twin screw wet granulation: effect of process and formulation variables on powder caking during production, Int. J. Pharm. 496 (2) (2015) 571–582.
[20] M. Chen, et al., Caking of crystals: characterization, mechanisms and prevention, Powder Technol. 337 (2018) 51–67.
[21] W. Pietsch, An interdisciplinary approach to size enlargement by agglomeration, Powder Technol. 130 (1) (2003) 8–13.
[22] S. Palzer, Agglomeration of pharmaceutical, detergent, chemical and food powders — Similarities and differences of materials and processes, Powder Technol. 206 (1) (2011) 2–17.
[23] M.-J. Colbert, M. Grandbois, N. Abatzoglou, Identification of inter-particular forces by atomic force microscopy and how they relate to powder rheological properties measured in shearing tests, Powder Technol. 284 (2015) 396–402.
[24] B.J. Ennis, G. Tardos, R. Pfeffer, A microlevel-based characterization of granulation phenomena, Powder Technol. 65 (1) (1991) 257–272.
[25] K. Nishii, et al., Pressure swing granulation, a novel binderless granulation by cyclic fluidization and gas flow compaction, Powder Technol. 74 (1) (1993) 1–6.
[26] V. Vivacqua, M. Ghadiri, Modelling of auto-agglomeration of cohesive powders, Chem. Eng. Res. Des. 133 (2018) 137–141.
[27] H.S. Kahrizsangi, D. Barletta, M. Poletto, Mechanical properties of agglomerates produced by the mechanical vibration of cohesive powders, Kona Powder Part. J. 33 (2016) 287–295.
[28] E. DesRosiers Lachiver, et al., Insights into the role of electrostatic forces on the behavior of dry pharmaceutical particulate systems, Pharm. Res. 23 (5) (2006) 997–1007.
[29] R.E. Gordon, A.I. Amin, Crystallization of Buprofen, 1984.
[30] N. Rasenack, B.W. Müller, Properties of Ibuprofen crystallized under various conditions: a comparative study, Drug Dev. Ind. Pharm. 28 (9) (2002) 1077–1089.
[31] M. Zhang, et al., Crystal engineering of ibuprofen compounds: from molecule to crystal structure to morphology prediction by computational simulation and experimental study, J. Cryst. Growth 467 (2017) 47–53.
[32] M.H. Shariare, et al., Influence of solvent on the morphology and subsequent comminution of Ibuprofen crystals by air jet milling, J. Pharm. Sci. 101 (3) (2012) 1108–1119.
[33] D. Hooper, et al., Effects of crystal habit on the sticking propensity of ibuprofen-a case study, Int. J. Pharm. 531 (1) (2017) 266–275.
[34] Malvern, Morphologi G3 User Manual, 2013.
[35] V.S. Kulkarni, C. Shaw, Chapter 11 - miscellaneous physical, chemical, and microbiological test methods, in: V.S. Kulkarni, C. Shaw (Eds.), Essential Chemistry for Formulators of Semisolid and Liquid Dosages, Academic Press, Boston, 2016, pp. 193–221.
[36] A. Zarrebini, et al., Tribo-electrification of powders due to dispersion, Powder Technol. 250 (2013) 75–83.
[37] S. Naik, et al., Quantification of tribocharging of pharmaceutical powders in V-Blenders: experiments, multiscale modeling, and simulations, J. Pharm. Sci. 105 (4) (2016) 1467–1477.
[38] R.G. Wilson, Vacuum thermionic work functions of polycrystalline Be, Ti, Cr, Fe, Ni, Cu, Pt, and Type 304 stainless steel, J. Appl. Phys. 37 (6) (1966) 2261–2267.
[39] T.T.H. Nguyen, et al., Precision measurement of the growth rate and mechanism of ibuprofen {001} and {011} as a function of crystallization environment, CrystEngComm 16 (21) (2014) 4568–4586.
[40] H.A. Garekani, et al., Crystal habit modifications of ibuprofen and their physicomechanical characteristics, Drug Dev. Ind. Pharm. 27 (8) (2001) 803–809.
[41] H. Cano, N. Gabas, J.P. Canselier, Experimental study on the ibuprofen crystal growth morphology in solution, J. Cryst. Growth 224 (3) (2001) 335–341.
[42] S. Gates-Rector, T. Blanton, The powder diffraction file: a quality materials characterization database, Powder Diffract. 34 (4) (2019) 352–360.
[43] E. Dudognon, et al., Evidence for a new crystalline phase of Racemic Ibuprofen, Pharm. Res. 25 (12) (2008) 2853–2858.
[44] Z. Jian, W. Hejing, The physical meanings of 5 basic parameters for an X-ray diffraction peak and their application, Chin. J. Geochem. 22 (1) (2003) 38–44.
[45] M. Birch, I. Marziano, Understanding and avoidance of agglomeration during drying processes: a case study, Org. Process. Res. Dev. 17 (10) (2013) 1359–1366.
[46] F. Fichtner, et al., Effect of preparation method on compactability of paracetamol granules and agglomerates, Int. J. Pharm. 336 (1) (2007) 148–158.
[47] H. Masuda, K. Gotoh, Performance evaluation of dry dispersers, Adv. Powder Technol. 6 (4) (1995) 305–315.
[48] W.R. Harper, Contact and Frictional ELectrification, Clarendon P, Oxford, 1967.
[49] S. Matsusaka, H. Masuda, Electrostatics of particles, Adv. Powder Technol. 14 (2) (2003) 143–166.
[50] S. Matsusaka, et al., Triboelectric charging of powders: a review, Chem. Eng. Sci. 65 (22) (2010) 5781–5807.
[51] M. Ghori, B. Conway, Triboelectrification of pharmaceutical powders: a critical review, Br. J. Pharm. 3 (1) (2018).
[52] R. Mukherjee, et al., A Simplex Centroid Design to Quantify Triboelectric Charging in Pharmaceutical Mixtures, J. Pharm. Sci. 109 (5) (2020) 1765–1771.
[53] N.M. Ahfat, et al., An exploration of inter-relationships between contact angle, inverse phase gas chromatography and triboelectric charging data, Eur. J. Pharm. Sci. 9 (3) (2000) 271–276.
[54] S. Wang, et al., Molecular surface functionalization to enhance the power output of triboelectric nanogenerators, J. Mater. Chem. A 4 (10) (2016) 3728–3734.
[55] L. Samiei, et al., The influence of electrostatic properties on the punch sticking propensity of pharmaceutical blends, Powder Technol. 305 (2017) 509–517.
[56] J. Eilbeck, et al., Effect of contamination of pharmaceutical equipment on powder triboelectrification, Int. J. Pharm. 195 (1) (2000) 7–11.
[57] K.C. Pingali, et al., An observed correlation between flow and electrical properties of pharmaceutical blends, Powder Technol. 192 (2) (2009) 157–165.
[58] F.J. Muzzio, A. Alexander, Scale Up of Powder- Blending Operations, 2005.